

MICROSTRUCTURAL EFFECTS IN ABRASIVE WEAR

Quarterly Progress Report
for the period 15 June 1978 - 15 September 1978

Nicholas F. Fiore, Joseph P. Coyle, Stephen Udvardy and
William Konkel

Department of Metallurgical Engineering and Materials Science
Notre Dame, IN 46556

NOTICE

This report was prepared as an account of work sponsored by the United States Government. Neither the United States nor the United States Department of Energy, nor any of their employees, nor any of their contractors, subcontractors, or their employees, makes any warranty, express or implied, or assumes any legal liability or responsibility for the accuracy, completeness, or usefulness of any information, apparatus, product or process disclosed or represents that its use would not infringe privately owned rights.

NOTICE
This report was prepared as an account of work sponsored by the United States Government. Neither the United States nor the United States Department of Energy, nor any of their employees, nor any of their contractors, subcontractors, or their employees, makes any warranty, express or implied, or assumes any legal liability or responsibility for the accuracy, completeness or usefulness of any information, apparatus, product or process disclosed, or represents that its use would not infringe privately owned rights.

1 October 1978

Prepared for

U. S. Department of Energy
Under Contract No. EF-77-S-02-4246

E.P
DISTRIBUTION OF THIS DOCUMENT IS UNLIMITED

DISCLAIMER

This report was prepared as an account of work sponsored by an agency of the United States Government. Neither the United States Government nor any agency Thereof, nor any of their employees, makes any warranty, express or implied, or assumes any legal liability or responsibility for the accuracy, completeness, or usefulness of any information, apparatus, product, or process disclosed, or represents that its use would not infringe privately owned rights. Reference herein to any specific commercial product, process, or service by trade name, trademark, manufacturer, or otherwise does not necessarily constitute or imply its endorsement, recommendation, or favoring by the United States Government or any agency thereof. The views and opinions of authors expressed herein do not necessarily state or reflect those of the United States Government or any agency thereof.

DISCLAIMER

Portions of this document may be illegible in electronic image products. Images are produced from the best available original document.

ABSTRACT

This project is directed toward correlating low-stress and gouging abrasive wear to microstructure in a series of alloy white irons and Co-base powder metallurgy (PM) alloys. In this quarter, additional tests have shown that low-stress abrasion resistance increases in a general way with hardness, whereas gouging wear resistance correlates to a significantly lesser extent. For gouging wear in particular, increasing hardness, carbon and alloy content are inefficient means to increase wear resistance.

Low-stress rubber wheel abrasive tests (RWAT) have been conducted with unused and used SiO_2 and Al_2O_3 , and sample weight loss and abrasive size degradation have been monitored. Relatively small changes in abrasive size distribution are found to be associated with marked differences in sample weight loss. Microtopographic analysis of the wear scars generated with all four types of abrasive indicate that wear-resistant alloys exhibit smoother wear scars.

In gouging wear or in low-stress wear against SiO_2 , maximum wear resistance is found at intermediate carbide volume fractions (v_f) and matrix alloy contents. For low-stress testing against Al_2O_3 , wear resistance increases linearly with v_f .

CONTENTS

ABSTRACT	i
1. OBJECTIVE AND SCOPE	1
2. TASKS AND PROGRESS	1
3. SUMMARY	22
4. PERSONNEL	23
LIST OF TABLES	24
LIST OF FIGURES	25

1. OBJECTIVE AND SCOPE

This work is directed at establishing quantitative relations between micro-structure and wear resistance of low-to-high Cr white irons (ASTM Series 532) and Co-base powder metallurgy (PM) alloys commonly used in coal conversion processes. The research involves study of gouging wear resistance, such as is necessary in mining operations, and low-stress abrasion resistance, such as required in coal and coal-product handling and transfer operations. The project has both applied and basic aspects. On the applied side, the establishment of the optimum micro-structures for wear resistance will allow (and is already beginning to allow) design engineers to make more effective decisions regarding candidate alloys for coal-related processes. From the basic viewpoint, the establishment of a better understanding of the physical and mechanical metallurgy of wear may lead in the longer run to the development of more economical and effective wear-resistant alloys.

The project has been in existence for about 18 months, during which time most of the testing and analysis has been conducted on the white irons. The majority of this, the sixth project quarterly report, is devoted to test results on the Co-base PM alloys.

2. TASKS AND PROGRESS

2.1 Task I - Preparation of Test Matrix

Task completed 6 June 1977.

2.2 Task II - Preparation of Materials

Task completed 15 March 1978.

The white iron and Co-base alloy materials have been obtained. The compositions, heat treatments and microstructures of the white irons have been discussed in the quarterly report, COO-4246-4, and a similar discussion for the

Co-base alloys has been given in the last quarterly report, COO-4246-5.

2.3 Task III - Wear Testing

2.3.1 Co-base PM Alloy Test Matrix

The six Co-base alloys chosen, whose chemical compositions are listed in Table I, are among the most erosion and erosion-corrosion resistant materials commercially available. In addition to being commercially relevant, the series of alloys comprise an interesting system for study since they span a range of increasing carbide volume fraction in matrices of increasing solid solution strengthener content (Table II).

2.3.2 Rubber-Wheel Abrasion Testing

2.3.2.1 The Abrasive and the RWAT

The RWAT has been developed as a test for low-stress abrasion, a process during which, by definition, the abrasive remains unchanged. Preliminary tests, as reported in quarterly COO-4246-3, indicated that in fact both SiO_2 and Al_2O_3 abrasive degraded in size during testing. The SiO_2 abrasive, of average mesh size 50-70, broke down in such a manner that substantial amounts (~20% of the total abrasive mass) of 70-100 mesh fine particles were created. The Al_2O_3 , having a bi-modal size distribution peaking at 60 and 80 mesh broke down to a much lesser extent. Surprisingly, the SiO_2 , which degraded markedly in size, lost only about 10 percent of its abrasiveness against 1020 steel, whereas the Al_2O_3 lost almost 50% of its abrasiveness. These preliminary tests indicated that RWAT test results must be interpreted in light of target and abrasive behavior.

Consequently a RWAT program was instituted in which triplicate samples of each Co-base PM alloy was run against unused SiO_2 , "used" SiO_2 (i.e. SiO_2 broken down by a previous run) unused Al_2O_3 and used Al_2O_3 . The same analyses for the unused, used-once and used-twice forms of each abrasive are shown in Figures 1 and 2. The break-down of the SiO_2 after one test is evident. A comparable additional

Table I.
Chemical Analysis of Co-base PM Alloys

	#6	#6HC	#19	#98M2	#3	#Star J
B	.49	.49	.22	.66	.49	.27
C	1.49	1.94	1.88	2.12	2.52	2.67
Co	Bal	Bal	Bal	Bal	Bal	Bal
Cr	28.99	28.99	30.17	30.57	30.91	31.57
Fe	1.46	1.46	1.92	3.09	2.29	.32
Mo	.32	.32	--	.24	.35	.02
Mn	.13	.13	0.65	.23	<.1	.58
Ni	2.13	2.13	1.42	4.04	2.20	1.34
Si	.92	.92	--	.51	.51	.34
V	--	--	--	3.82	--	<.01
W	4.96	4.96	10.37	17.15	11.78	16.94

Table II
Features of the Co-base Powder Metallurgy Alloys

	Type	Microstructure
1. #6	Low carbide vol. fract.	Low solid solution strengthener content.
2. #6HC	High carbide vol. fract.	Low solid solution strengthener content.
3. #19	High carbide vol. fract.	Moderate solid solution strengthener content.
4. #98M2	Very high carbide vol. fract.	Very high solid solution strengthener content.
5. #3	Very high carbide vol. fract.	High solid solution strengthener content.
6. #Star-J	Very high carbide vol. fract.	High solid solution strengthener content.

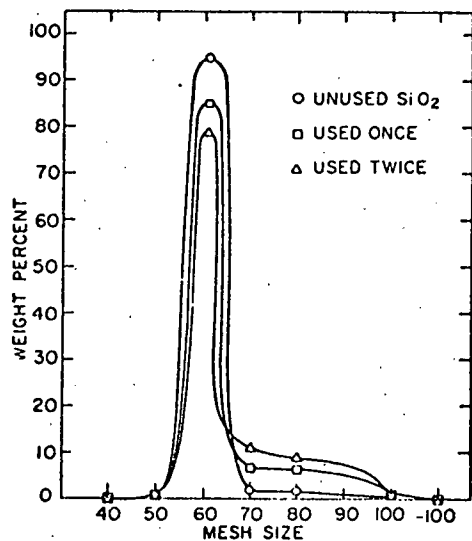


Figure 1. Sieve analysis of SiO_2 abrasive (unused, used once, used twice in RWAT tests on Co-base PM alloys).

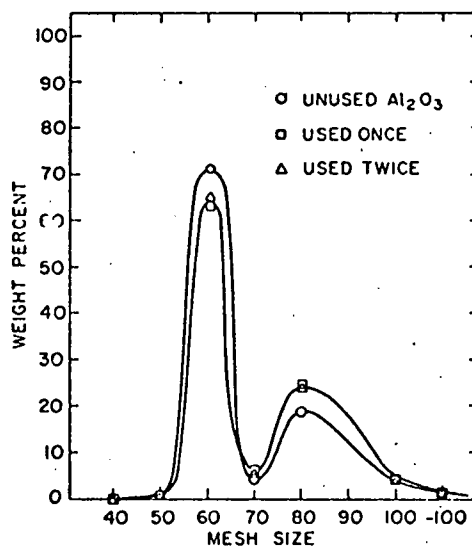


Figure 2. Sieve analysis of Al_2O_3 abrasive (unused, used once, used twice in RWAT tests on Co-base PM alloys).

breakdown occurs during the second test, so that after the abrasive has been used twice about 20% of it falls into -70 size classes. The Al_2O_3 breaks down to a lesser extent during its first usage, and does not break down further during the second usage.

2.3.2.2 RWAT Results - Unused and Used SiO_2

Figure 3 shows RWAT weight loss against alloy macrohardness (R_c) for the Co-base alloys tested against unused and used SiO_2 . Shown in the figure are least-square straight lines fit to the unused and used SiO_2 data. The wear-hardness correlation coefficient r is 0.78 for unused SiO_2 and 0.88 for used SiO_2 . The theory of abrasive indicates* that weight loss should vary as $(\text{hardness})^{-1}$. It has been found in this program that the data follow the direct wear-hardness correlation at least as well as the reciprocal hardness correlation, so for the purposes of simplicity the data are presented in direct form. These present data, as have previous sets, indicate that hardness provides a semi-quantitative gage of wear resistance for the RWAT.

It is evident from Figure 3 that the SiO_2 abrasive loses about 50 percent of its abrasiveness after one use. This effect is seen more clearly in Figure 4, in which the weight loss data are presented in histogram form.

The results with unused and used SiO_2 help to account for the strong differences of opinion concerning wear test results obtained at various laboratories. Small changes in abrasive behavior produce unpredictable changes in abrasiveness. As mentioned previously, the break-down of SiO_2 did not decrease its abrasiveness against 1020 steel; however, a marked reduction occurs against the Co-base alloys.

In a more positive vein, data with the various abrasives present the opportunity for gaining insight as to the material attrition processes governing low-stress

* See for example E. Rabinowicz, Friction and Wear of Materials (Wiley, New York, 1964) p. 168.

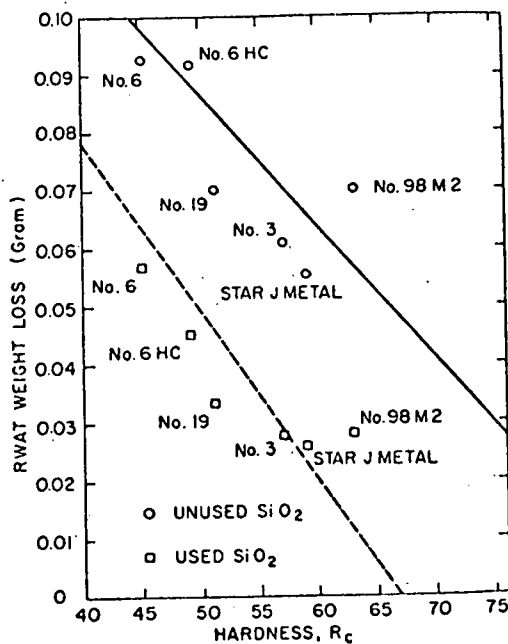


Figure 3. RWAT weight loss of Co-base PM alloys as a function of alloy hardness, Rockwell R_c . (Unused and used SiO_2 abrasive).

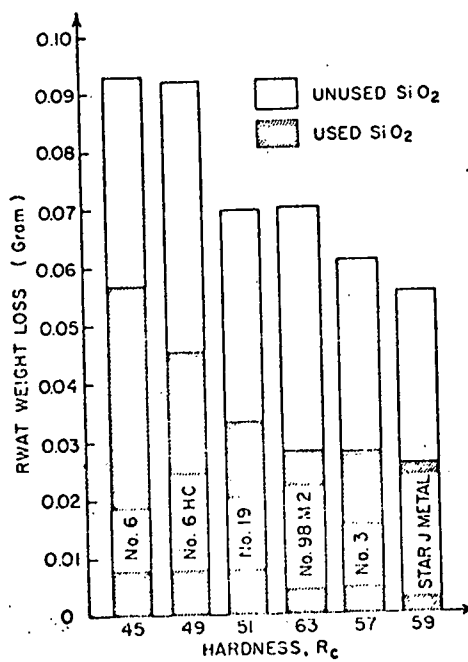


Figure 4. Histogram of RWAT weight loss for Co-base PM alloys tested against unused and used SiO_2 .

abrasion of these materials if a correlation can be made between the relatively small changes in abrasive characteristics and the large changes in weight loss. For example, the abrasive may be degraded into small particles by the fragmenting of sharp corner particles from the parent grain (although grains of this particular abrasive are semi-rounded rather than markedly angular). The significant loss of abrasiveness in this case would suggest that micro-machining processes govern low-stress wear.

2.3.2.3 RWAT Results - Unused and Used Al_2O_3

As is evident from the plots and histograms of Figures 5 and 6, RWAT testing with Al_2O_3 produces clear differences from testing with SiO_2 . In the first place, the correlation between wear and hardness is extremely good for both the unused ($r = 0.94$) and the used ($r = 0.96$) abrasive. This is somewhat surprising in that a rule-of-thumb* in designing for wear resistance is that hardness is an effective design parameter until the abrasive hardness exceeds target hardness. At this point, processing to increase target hardness is considered inefficient. The Al_2O_3 abrasive, with hardness about 2000 KHN is substantially harder than even the hardest of the PM alloys with M_7C_3 hardness about 1800 KHN and yet gains in wear resistance are evident as hardness is increased. The gains are also evident for the case of SiO_2 , about 800 KHN, but this is not surprising because the abrasive and target hardnesses are more similar in this case.

The common model* of abrasive wear is based on a situation in which an infinitely hard conical abrasive particle partially penetrates the surface of a target of hardness H and removes a furrow of matter as it slides along the surface. These data show that, as many others have seen that hardness may be a useful parameter in designing for wear resistance, but that the usefulness should not be taken as an indication that the model is valid.

*E. Rabinowicz, op. cit, p. 172.

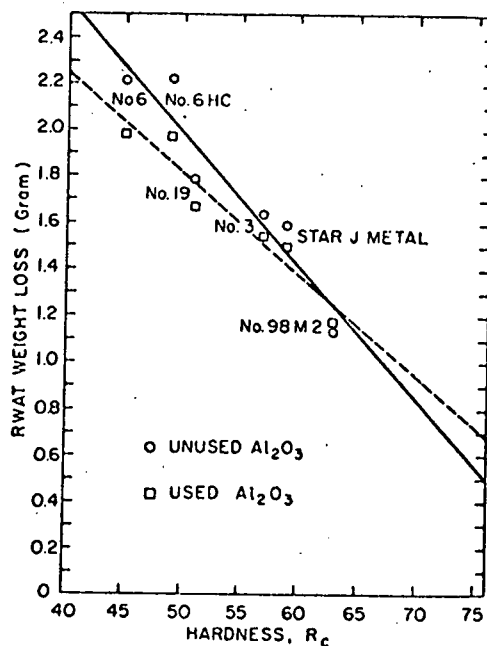


Figure 5. RWAT weight loss of Co-base PM alloys as a function of alloy hardness, Rockwell C. (Unused and used Al_2O_3 abrasive).

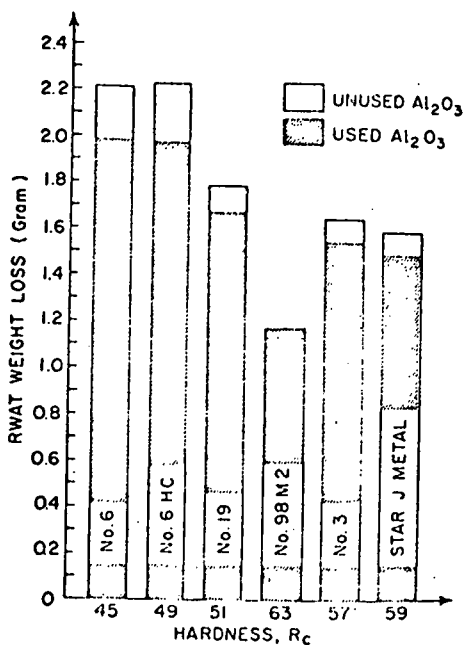


Figure 6. Histogram of RWAT weight loss for Co-base PM alloys tested against unused and used Al_2O_3 .

The data also show that abrasive size degradation appears to have less influence on the abrasiveness of the Al_2O_3 than on the SiO_2 . The differences in weight loss observed for the unused and used Al_2O_3 are small. This result, as well as the others mentioned for the SiO_2 and Al_2O_3 abrasives is discussed further under Task V, Analysis of Data.

2.3.3 Gouging Abrasion Testing

The GAWT tests results for the six Co-base PM alloys were presented in the last quarterly (COO-4246-5). They are summarized here in Figures 7 (GAWT weight loss vs R_c) and Figure 8 (GAWT data in histogram form). The previous RWAT data lead to the general conclusion that low-stress abrasion resistance improves as alloy cost increases. It is evident that this trend is not as clear for gouging abrasion resistance. The poorer correlation between wear resistance and alloy content in the case of gouging wear is borne out in Figure 7, with a wear-hardness correlation coefficient r of 0.65, as contrasted with the necessary value of 0.8 for significant correlation as defined in COO-4246-3.

2.4 Task IV - Wear Scar and Microstructure Characterization

2.4.1 Optical and Quantitative Metallography of Co-base Alloys

The optical and quantitative metallographic (QTM) analysis of the PM alloys have been described in COO-4246-5. The alloys consist of an array of carbides uniformly distributed in a FCC Co-base matrix. In general the carbides are of type $M_7\text{C}_3$, where M is largely Cr. The most highly alloyed material contain about 10 volume percent $M_6\text{C}$ carbides, where M corresponds to W, Co and Cr. The QTM results are re-summarized in Table III. Total carbide volume fraction, v_f , increases from 34 to 57% across the range of alloys, whereas carbide size is about constant with the exception of alloy #98M2 which has smaller carbides.

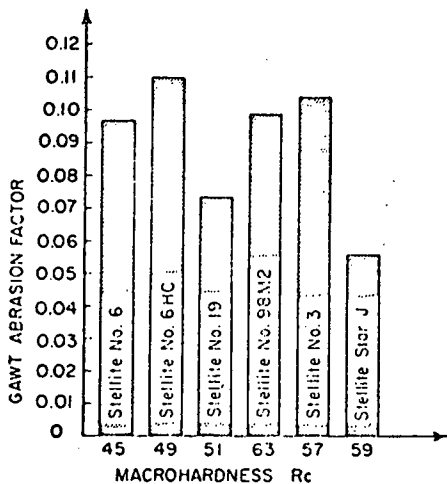


Figure 7. GAWT weight loss of Co-base PM alloys. Carbide volume fraction and/or matrix solid-solution strengthener content increase left to right.

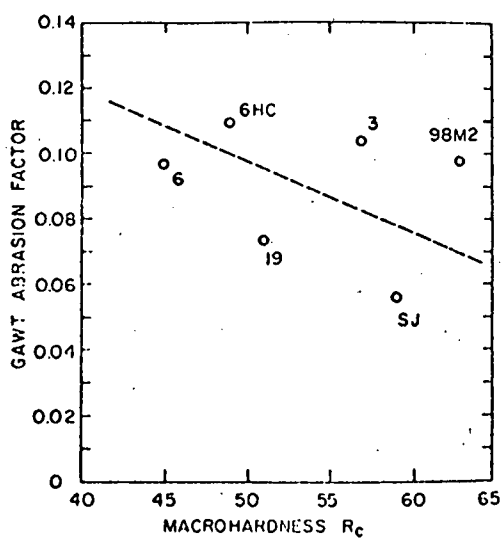


Figure 8. GAWT abrasion factor of Co-base PM alloys as a function of Rockwell C hardness.

Table III
Quantitative Metallographic Results for Co-base PM Alloys

Alloy	<u>Volume Fraction, Percent</u>				<u>Projected Carbide</u>		
	Porosity	Cr_7C_3	M_6C	Total Carbides	σ_v Std. Dev. (%)	Length per Unit Area (cm^{-1})	σ_L Std. Dev. (cm^{-1})
No. 6	1.8	33.8	0	33.8	2.1	0.010	.0007
No. 6HC	1.6	39.5	0	39.5	3.5	0.013	.0013
No. 19	1	37.4	0	37.4	1.4	0.012	.0006
No. 98M2	0	43.6	13	56.6	2.1	0.019	.0004
No. 3	0	46.3	8.9	55.2	5.3	0.011	.0004
Star J-Metal	0	41.0	8.9	49.9	1.3	0.014	.0002

2.4.2 Wear Scar Microtopography of Co-base PM Alloys

Wear scar micro-profilometry is conducted at the Inland Steel Research Laboratories. The measurements are made with a Sloan profilometer having a 0.0127 mm diameter diamond stylus. Detailed descriptions of the measuring technique and of the computer analysis have been given in COO-4246-4 and 5. In summary, the techniques and analysis produce three measures of roughness:

1. $P(I)$ - The "actual" surface profile. A composite of both coarse and fine topographical features.
2. $C(I)$ - The centerline profile, which consists of the coarse features only
3. $R(D) = P(I) - C(I)$ -- The residual topography which consists of the fine features alone.

The analysis to date has been concentrated on the relation of $R(I)$ to wear behavior. There are three quantitative measures of $R(C)$, as defined in the last quarterly. These are:

1. AA, the average displacement from centerline.
2. RMS, the rms roughness.
3. PPI, the number of peaks per inch scanned.

The RWAT wear scars produced during the tests with unused and used SiO_2 and Al_2O_3 have been analyzed according to the above procedure. In all cases the surface trace was obtained near the top of the wear scar, where abrasive first meets target. Although the most relevant material loss mechanisms may be operating further down the scar, attention is focused at the top region for these initial measurements because of the greater ease of obtaining reproducible data. The profilometry to-date has involved considerable effort in perfecting the Inland experimental system with on-line computer analysis to our needs, so the simplest procedures are being employed at this stage.

The microprofilometry results are given in Figures 9-20. The figures are presented in sets of three (AA, RMS, PPI) for each of the four RWAT conditions: unused SiO_2 , used SiO_2 , unused Al_2O_3 , used Al_2O_3 . The topography-wear correlation coefficients are listed in each caption, and they indicate, in a general way, that the more resistant a material, the smoother will be its wear scar. The exception to this qualitative rule is found for used Al_2O_3 , in which no statistically significant correlation exists between wear resistance and topography.

At least three problems must be addressed before these or other topographic results can be interpreted:

1. Is the Inland Steel data analysis procedure relevant to our purposes?

For example, it may be more important to concentrate on the coarser detail $C(I)$ than $R(I)$, given the scale of the wear scar features.

At the other extreme is the question:

2. Are the three measures of microtopography, (AA, RMS, PPI), fine enough to resolve relevant features?

3. What regions of the wear scars provide useful information about the relevant material attrition mechanisms?

The general correlations found thus far indicate that it is worthwhile to consider these questions. A series of scanning electron microscopy (SEM) studies will be undertaken to define the scale of the topographic information of interest. Given the number of wear samples already in existence, the SEM studies will occupy a substantial portion of effort during the next quarter.

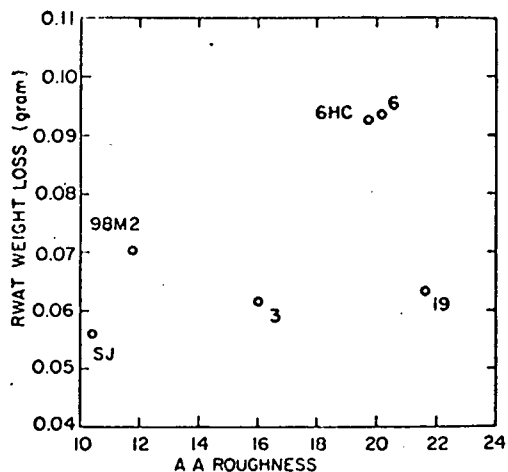


Figure 9. RWAT weight loss vs AA microtopography. (Unused SiO_2 - r not significant.)

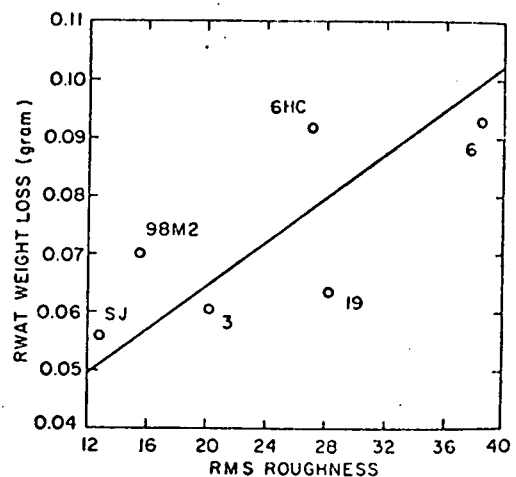


Figure 10. RWAT weight loss vs. RMS microtopography. (Unused SiO_2 - $r = 0.62$).

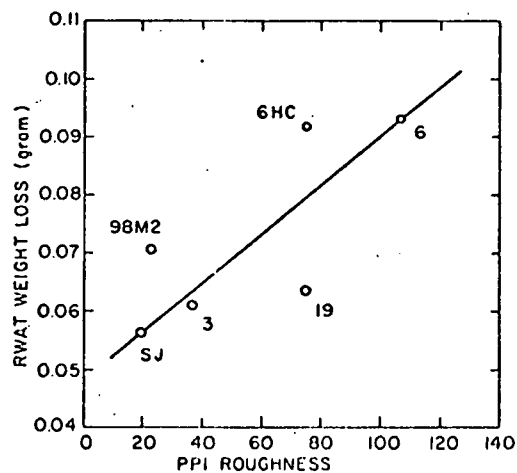


Figure 11. RWAT weight loss vs PPI microtopography. (Unused SiO_2 - $r = 0.71$).

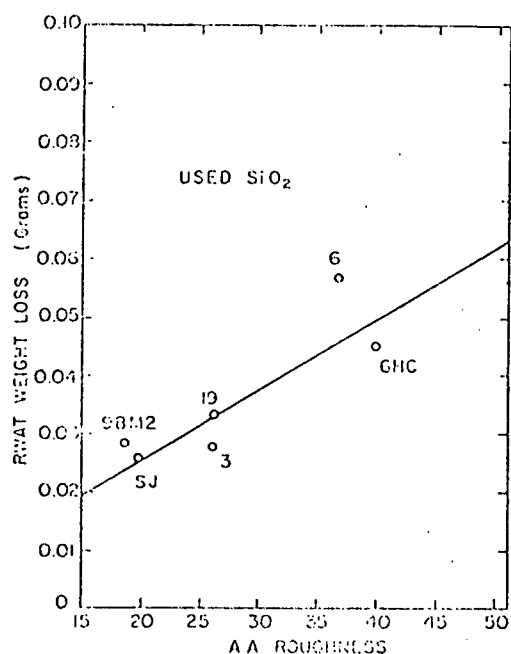


Figure 12. RWAT weight loss vs AA microtopography. (Used SiO_2 - $r = 0.88$).

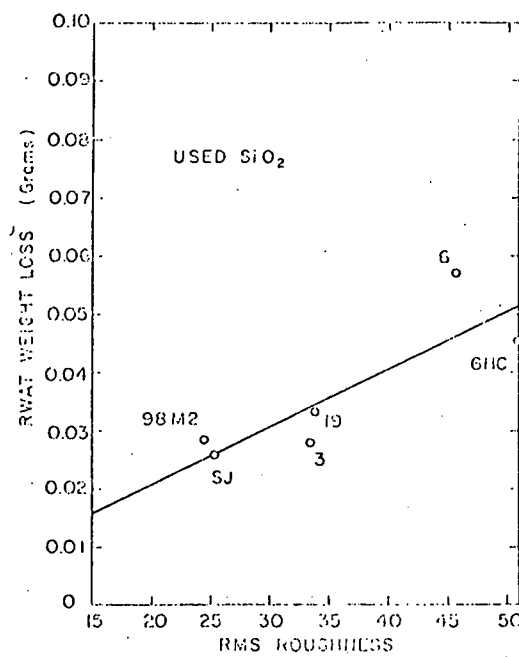


Figure 13. RWAT weight loss vs RMS microtopography. (Used SiO_2 - $r = 0.86$).

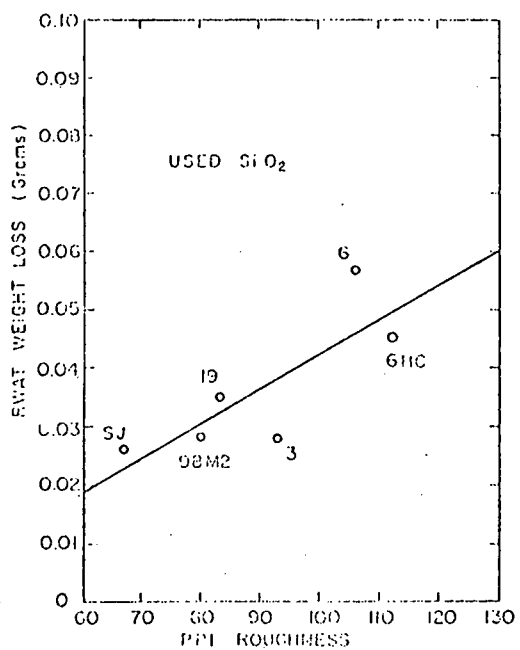


Figure 14. RWAT weight loss vs PPI microtopography (Used SiO_2 - $r = 0.81$).

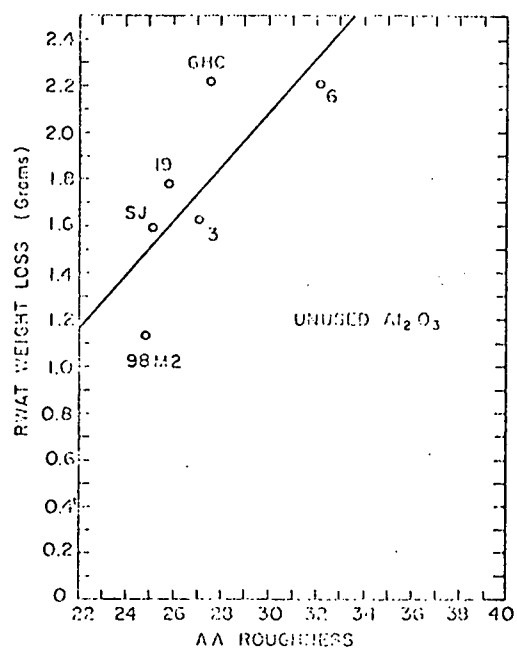


Figure 15. RWAT weight loss vs AA microtopography. (Unused Al_2O_3 - $r = 0.75$).

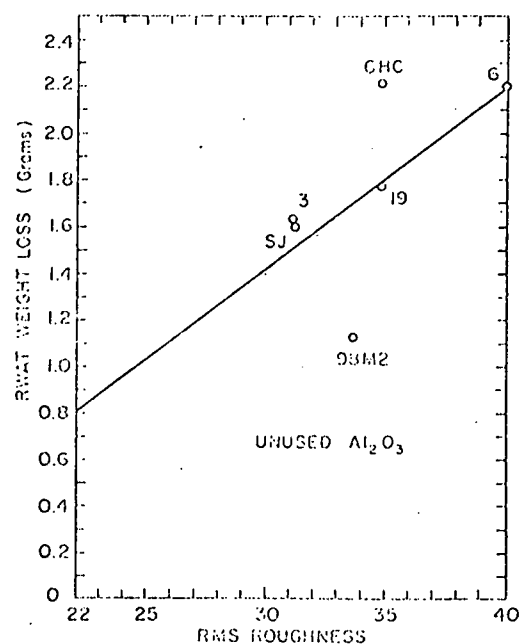


Figure 16. RWAT weight loss vs RMS microtopography (Unused Al_2O_3 - $r = 0.61$).

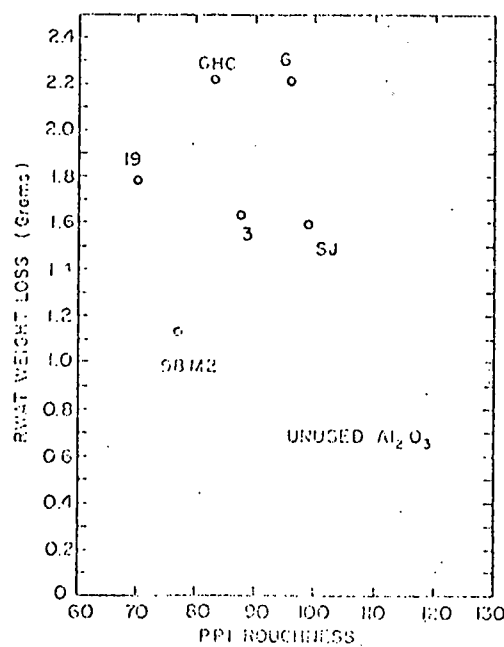


Figure 17. RWAT weight loss vs PPI microtopography. (Unused Al_2O_3 - r not significant)

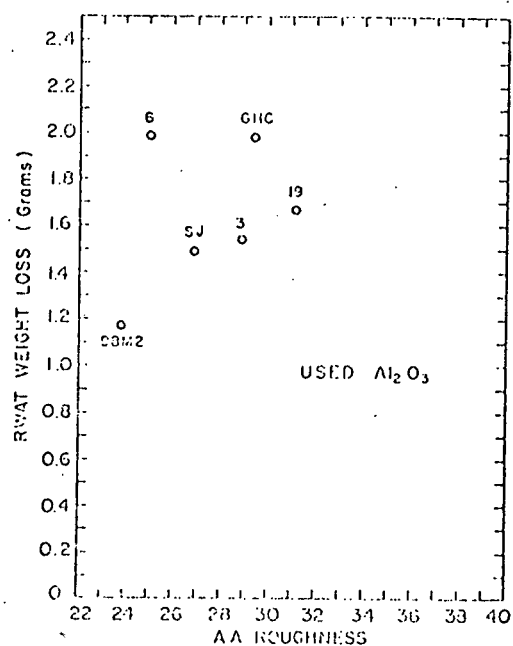


Figure 18. RWAT weight loss vs AA microtopography. (Used Al_2O_3 - r not significant).

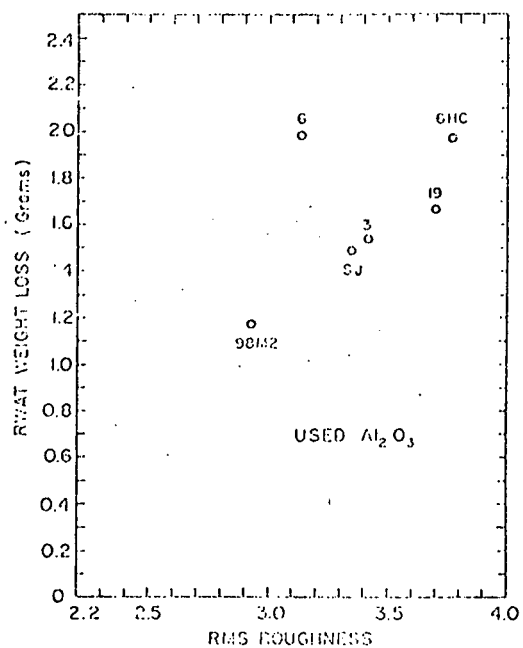


Figure 19. RWAT weight loss vs RMS microtopography. (Used Al_2O_3 - r not significant).

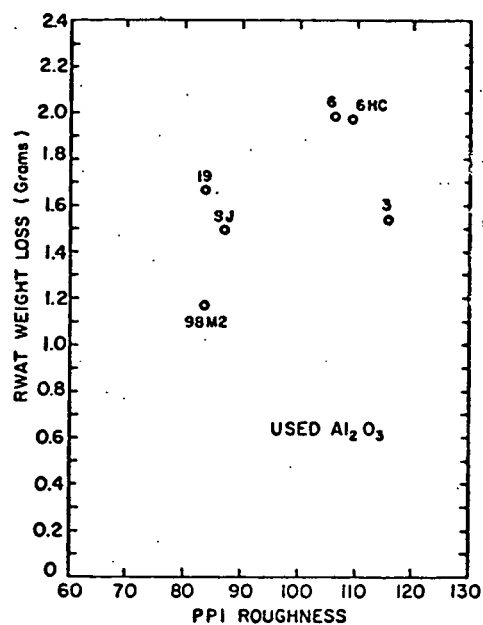


Figure 20. RWAT weight loss vs PPI microtopography. (Used Al_2O_3 - r not significant).

2.5 Task V - Analysis of Data

2.5.1 General Behavior of the Co-base PM Alloys

The GAWT, RWAT and microtopographic test data on the Co-base alloys may be summarized in five general statements:

1. GAWT weight loss decreases, in a very general sense, as hardness, carbon and alloy content increase.
2. Alloying appears to be an expensive and inefficient means of increasing gouging wear resistance.
3. RWAT weight loss decreases as hardness, carbon and alloy content increase. This general trend holds for unused and used Si O_2 .
4. Hardness is an unsatisfactory parameter for characterizing the abrasive in a low-stress wear situation. The manner in which an abrasive degrades during a test may give insight to material attrition mechanism.
5. In low-stress abrasion, abrasion-resistant alloys are characterized by smoother wear scars.

These qualitative statements, especially the two regarding topography and target-abrasive interactions provide the basis for mechanistic studies of the wear process. The SEM program planned for the next quarter will involve study of both the wear scar and abrasive and should provide for the first time a coupling between the micro flow-fracture processes governing this form of wear and the macro wear data generated thus far.

2.5.2 Wear - Microstructure Correlations for the Co-base Alloys

A major object of the program is to use correlations between microstructure and wear to improve the understanding of wear. Although the analysis of the macroscopic wear data on the Co-base alloys is just beginning, several significant microstructural effects are evident.

The PM alloys comprise a family of increasing carbide fraction and increasing alloy (Cr + Ni + V + W) content. In Table IV are listed R_c hardnesses, carbide volume fractions and total alloying element contents normalized to alloy #6, the least-alloyed, lowest- v_f alloy. Since v_f and alloy content cannot be varied

Table IV
Normalized Carbide v_f and Alloy Content of PM Alloys

Alloy	#6	#19	#6HC	#Star-J	#3	#98MC
Hardness (R_c)	45	51	49	59	57	63
Normalized Carbide v_f	1.0	1.1	1.2	1.5	1.6	1.7
Normalized Alloy Content	1	1.7	1	2.6	2.0	3.5

independently in these commercial alloys, it is not possible to separate the respective contributions to alloy wear resistance. The difficulty is illustrated in Figures 21 through 24. When weight loss is plotted against either normalized v_f or alloy content, similar functional dependencies are observed. For the unused and used Al_2O_3 (Figures 23 and 24), weight loss decreases linearly with increasing v_f or alloy content.

Although the carbide and matrix effects may not be separated at this point, useful wear-structure generalizations are evident.

1. The similarity in the v_f dependencies for gouging and low-stress abrasion against SiO_2 may indicate that similar material attrition mechanisms govern both situations.
2. For wear resistance against the softer SiO_2 abrasive, an optimum alloy content/ v_f exists. Alloying beyond this point is not only wasteful, it is counterproductive.

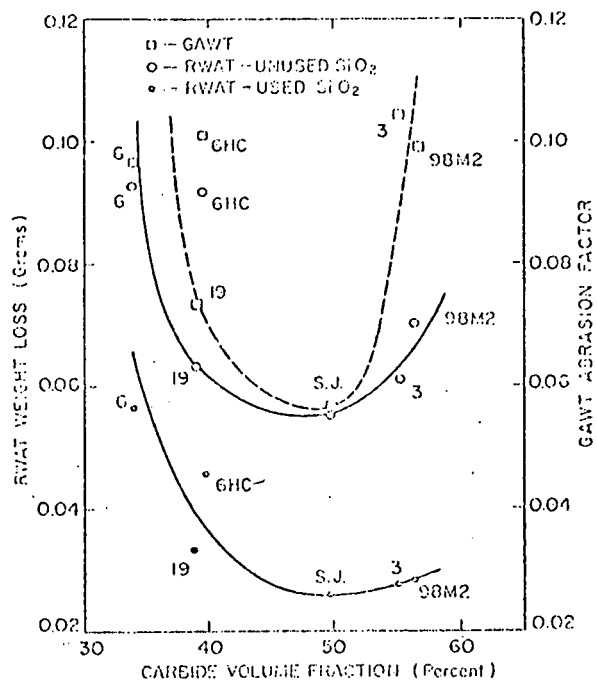


Figure 21. GAWT abrasion factor and RWAT weight loss (unused and used SiO_2) vs carbide v_f .

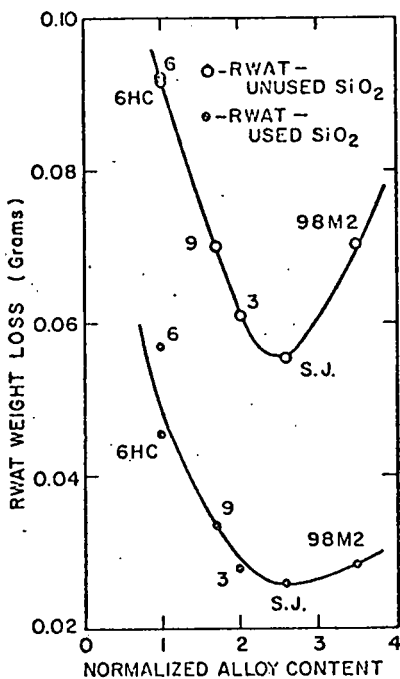


Figure 22. RWAT weight loss (unused and used SiO_2) vs normalized alloy content.

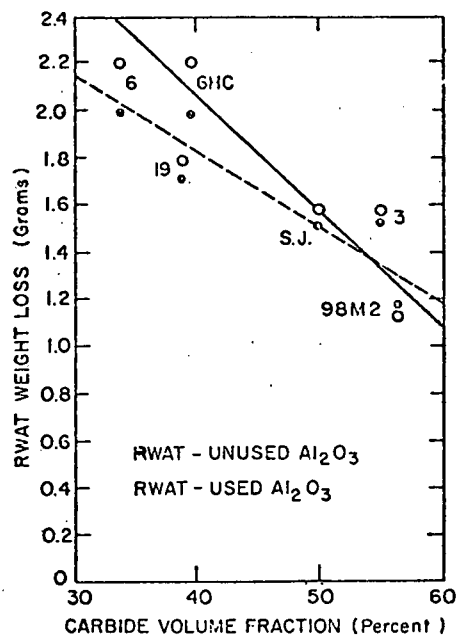


Figure 23. RWAT weight loss (unused and used Al_2O_3) vs carbide v_f .

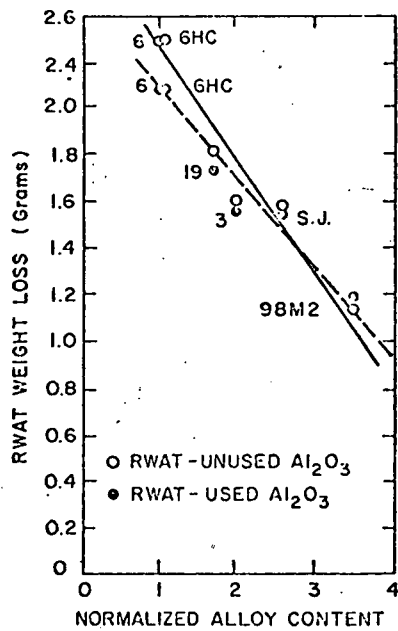


Figure 24. RWAT weight loss (unused and used Al_2O_3) vs normalized alloy content.

3. For wear resistance against the harder Al_2O_3 abrasive, increasing alloy content/ v_f is worthwhile.
4. In contrast to the results with 1020 steel, degradation of the SiO_2 causes a marked decrease in abrasiveness against the PM alloys, whereas degradation of the Al_2O_3 has little effect.

Tests have been proposed for a later phase of the project in which the effects of matrix alloy content and v_f on wear may be separated.

3. SUMMARY

During this quarter, emphasis has been placed on the study of abrasive-alloy content-carbide v_f interactions in low-stress abrasion of the PM alloys. The RWAT tests, followed by sieve analyses, indicate that both SiO_2 and Al_2O_3 abrasives degrade during the test. It appears that small changes in abrasive may bring about large changes in abrasiveness. Abrasive hardness is certainly not the only parameter governing wear, even in the low-stress case. SEM studies of the abrasive may provide insight as to which properties of the abrasive govern abrasiveness and which material attrition processes are operative during wear.

In a general way, target hardness is a usable indicator of wear resistance, although predictions based upon it may be in error by a factor of two or more.

The microtopography studies lead to the conclusion that more wear-resistant materials exhibit smoother wear scars. Before the topography data may be used to give insight to the wear process, the experimental procedure and computer analysis must be examined in conjunction with careful SEM studies of the wear scars.

Hardness of the PM alloys is not as satisfactory a gage of gouging wear resistance as it is of low-stress resistance. In either gouging wear or low-stress wear against SiO_2 optimum levels of alloying to increase matrix strength or v_f exist. Exceeding the optimum values is counterproductive. For the case of low-

stress wear against Al_2O_3 , wear resistance appears to increase in direct proportion to v_f .

4. PERSONNEL

The principal investigator, Dr. N. F. Fiore, and the co-principal investigator, Dr. T. Kosel, spent about one-third effort on the project during this summer quarter. The graduate research assistants, Mr. William Konkel and Mr. Stephen Udvardy, have devoted full-time to the work.

LIST OF TABLES

Table I. Chemical Analysis of Co-base PM Alloys

Table II. Features of the Co-base Powder Metallurgy Alloys

Table III. Quantitative Metallographic Results for Co-base PM Alloys

Table IV. Normalized Carbide v_f and Alloy Content of PM Alloys

LIST OF FIGURES

Fig. 1. Sieve analysis of SiO_2 abrasive (unused, used once, used twice in RWAT tests on Co-base PM alloys).

Fig. 2. Sieve analysis of Al_2O_3 abrasive (unused, used once, used twice in RWAT tests on Co-base PM alloys).

Fig. 3. RWAT weight loss of Co-base PM alloys as a function of alloy hardness, Rockwell R_c . (Unused and used SiO_2 abrasive).

Fig. 4. Histogram of RWAT weight loss for Co-base PM alloys tested against unused and used SiO_2 .

Fig. 5. RWAT weight loss of Co-base PM alloys as a function of alloy hardness, Rockwell C. (Unused and used Al_2O_3 abrasive).

Fig. 6. Histogram of RWAT weight loss for Co-base PM alloys tested against unused and used Al_2O_3 .

Fig. 7. GAWT weight loss of Co-base PM alloys. Carbide volume fraction and/or matrix solid-solution strengthener content increase left to right.

Fig. 8. GAWT abrasion factor of Co-base PM alloys as a function of Rockwell C hardness.

Fig. 9. RWAT weight loss vs AA microtopography. (Unused SiO_2 - r not significant).

Fig. 10. RWAT weight loss vs RMS microtopography. (Unused SiO_2 - $r = 0.62$).

Fig. 11. RWAT weight loss vs PPI microtopography. (Unused SiO_2 - $r = 0.71$).

Fig. 12. RWAT weight loss vs AA microtopography. (Used SiO_2 - $r = 0.88$).

Fig. 13. RWAT weight loss vs RMS microtopography. (Used SiO_2 - $r = 0.86$).

Fig. 14. RWAT weight loss vs PPI microtopography. (Used SiO_2 - $r = 0.81$).

Fig. 15. RWAT weight loss vs AA microtopography. (Unused Al_2O_3 - $r = 0.75$).

Fig. 16. RWAT weight loss vs RMS microtopography. (Unused Al_2O_3 - $r = 0.61$).

Fig. 17. RWAT weight loss vs PPI microtopography. (Unused Al_2O_3 - r not significant).

Fig. 18. RWAT weight loss vs AA microtopography. (Used Al_2O_3 - r not significant).

Fig. 19. RWAT weight loss vs RMS microtopography. (Used Al_2O_3 - r not significant).

Fig. 20. RWAT weight loss vs PPI microtopography. (Used Al_2O_3 - r not significant).

Fig. 21. GAWT abrasion factor and RWAT weight loss (unused and used SiO_2) vs carbide v_f .

Fig. 22. RWAT weight loss (unused and used SiO_2) vs normalized alloy content.

Fig. 23. RWAT weight loss (unused and used Al_2O_3) vs carbide v_f .

Fig. 24. RWAT weight loss (unused and used Al_2O_3) vs normalized alloy content.

DISTRIBUTION LIST

Mr. John J. Mahoney
Senior Contract Administrator
Contracts Management Office
DOE - Chicago Operations Office
9700 South Cass Avenue
Argonne, IL 60439
- 6 copies -

Dr. Thomas Cox
DOE - Fossil Energy Research
Room 4203
20 Massachusetts Avenue
Washington, D.C. 20545
- 3 copies -

Dr. Paul Scott
DOE - Fossil Energy Research
20 Massachusetts Avenue
Washington, D.C. 20545

Dr. Sam Schnedier
National Bureau of Standards
Washington, D.C. 20234

Dr. John Dodd
Climax Molybdenum Company
13949 West Colfax Avenue
Golden, CO 80401

Metals and Ceramics Information Center
Battelle-Columbus Laboratories
505 King Avenue
Columbus, OH 43201

Dr. J. L. Parks
Climax Molybdenum Research Lab.
1600 Huron Parkway
Ann Arbor, MI 48106

Dr. M. S. Bhat
Materials and Molecular Research
Bldg. 62 - Room 239
Lawrence Berkeley Laboratory
University of California
Berkeley, CA 94720

Mr. Howard Avery
69 Alcott
Mahwah, N.J. 07430

Dr. Kenneth Anthony
Stellite Division
Cabot Corporation
Kokomo, IN 46901

Dr. Stanley Wolf
Materials Science Program
Division of Basic Energy Sciences
DOE
Washington, D.C. 20545

Dr. Joseph Klein
Stellite Division
Cabot Corporation
Kokomo, IN 46901

Dr. Jerry L. Arnold
Research and Technology
Armco Steel Corporation
Middletown, OH 45043

Dr. R. C. Tucker
Union Carbide Corp.
1500 Polco Street
Indianapolis, IN 46224

Dr. Paul Swanson
Deere and Company Technical Center
3300 River Drive
Moline, IL 61265